Measurements of the superconducting fluctuations in optimally doped $BaFe_{2-x}Ni_xAs_2$ under high magnetic fields: probing the 3D-anisotropic Ginzburg–Landau approach

2014 Supercond. Sci. Technol. 27 075001

(http://iopscience.iop.org/0953-2048/27/7/075001)

IOP Publishing Superconductor Science and Technology
Supercond. Sci. Technol. **27** (2014) 075001 (9pp) doi:10.1088/0953-2048/27/7/075001

Measurements of the superconducting fluctuations in optimally doped $BaFe_{2-x}Ni_xAs_2$ under high magnetic fields: probing the 3D-anisotropic Ginzburg–Landau approach

R I Rey[1], A Ramos-Álvarez[1], C Carballeira[1], J Mosqueira[1], F Vidal[1], S Salem-Sugui Jr.[2], A D Alvarenga[3], Rui Zhang[4] and Huiqian Luo[4]

[1] LBTS, Facultade de Física, Universidade de Santiago de Compostela, E-15782 Santiago de Compostela, Spain
[2] Instituto de Fisica, Universidade Federal do Rio de Janeiro, 21941-972 Rio de Janeiro, RJ, Brazil
[3] Instituto Nacional de Metrologia Qualidade e Tecnologia, 25250-020 Duque de Caxias, RJ, Brazil
[4] Beijing National Laboratory for Condensed Matter Physics, Institute of Physics, Chinese Academy of Sciences, Beijing 100190, People's Republic of China

E-mail: j.mosqueira@usc.es

Received 4 February 2014, revised 2 April 2014
Accepted for publication 7 April 2014
Published 23 May 2014

Abstract
The superconducting fluctuations well inside the normal state of Fe-based superconductors were experimentally studied through the in-plane paraconductivity in several high-quality, optimally doped $BaFe_{2-x}Ni_xAs_2$ crystals. These measurements were performed in magnetic fields with amplitudes up to 14 T, and different orientations relative to the *c*-axis of the crystals ($\theta = 0°$, 53°, and 90°). The results allowed a stringent check of the applicability of a recently proposed Ginzburg–Landau approach for the fluctuating electrical conductivity of three-dimensional (3D) anisotropic materials in the presence of finite applied magnetic fields.

Keywords: Fe-based superconductors, transport properties, superconducting fluctuations

(Some figures may appear in colour only in the online journal)

1. Introduction

The high critical temperatures (T_c) of Fe-based superconductors (FeSC) and the unconventional mechanism for their superconductivity (with a pairing probably mediated by spin fluctuations and involving several bands) have generated enormous interest for these materials in the last few years [1]. A central aspect of their phenomenology is the effect of superconducting fluctuations around T_c [2]. Mainly due to the short coherence length and high-T_c values of these materials [1], these effects are enhanced with respect to conventional low-T_c superconductors. In fact, the Ginzburg number, which characterizes the width of the critical fluctuation region around T_c, is in FeSC at half the level found in conventional low-T_c superconductors and high-T_c cuprates [3].

In addition to their intrinsic interest, superconducting fluctuation effects are a very useful tool for characterizing the nature of a superconducting transition and obtaining material parameters [2]; different works have already addressed their study in FeSC through observables like magnetization, specific heat, or electric conductivity [3–23]. However, some fundamental aspects of the phenomenology of the fluctuation effects in these materials are still debated. One of them is their dimensionality. In these materials, the transverse coherence length amplitude $\xi_c(0)$ is close to the Fe layer's periodicity length, *s*. Thus, depending on the particular compound

studied, some works report a two-dimensional (2D) behavior [3, 10, 20] similar to the one found in highly anisotropic high-T_c cuprates [24], while others find three-dimensional (3D) characteristics [4–7, 11, 12, 14–16, 19, 21–23] or even a 3D–2D transition [8, 13, 18] when increasing the temperature above T_c (as in optimally doped $YBa_2Cu_3O_{7-\delta}$) [24][5]. Besides, it was recently reported that the fluctuating electrical conductivity above T_c of clean LiFeAs crystals seems to follow a well defined 2D behavior in both its amplitude and reduced-temperature dependence, despite the fact that for this compound, $\xi_c(0) \approx 1.6$ nm is much larger than the periodicity length of the Fe-layers ($s = 0.636$ nm) [20]. This surprising result led the authors of [20] to propose that in these multiband superconductors, the fluctuating pairs above T_c may be driven by a single 2D band. Other interesting issues that deserve attention are the possible presence of *phase fluctuations* (whose effect was possibly observed near T_c at low field amplitudes in the $SmFeAsO_{0.8}F_{0.2}$ [17], and also in members of the less anisotropic 122 family as $Ba_{1-x}K_xFe_2As_2$ [5] and $Ba(Fe_{1-x}Rh_x)_2As_2$ [25]), or the behavior of fluctuation effects in the short wavelength regime appearing at high reduced magnetic fields or temperatures.

To contribute to the understanding of the above mentioned-issues, we present detailed measurements of the fluctuation-induced in-plane electric conductivity ($\Delta\sigma_{ab}$) in several high-quality $BaFe_{2-x}Ni_xAs_2$ crystals with near-optimal doping levels ($x \approx 0.1$). These experiments were performed in magnetic fields (H) up to 14 T applied with different angles θ relative to the crystal's c-axis ($\theta = 0$, 53, and 90 degrees), thus extending previous measurements in the same compound with $H \perp ab$ up to 9 T [21, 22]. The large fields used here allow deep penetration into the so-called Prange fluctuation regime. These fields also allow us to perform a stringent check of the applicability of a recently proposed generalization of the classic Aslamazov–Larkin (AL) results to finite fields through a 3D-anisotropic Ginzburg–Landau (GL) approach [21]. In turn, the use of different magnetic field orientations provides an important consistency test of the analysis, and allows us to obtain precise information about the system dimensionality, basic superconducting parameters (as the coherence lengths and the anisotropy factor), and the angular dependence of the upper critical field, which is currently another debated issue in these materials [26].

2. Experimental details and results

We studied three $BaFe_{2-x}Ni_xAs_2$ single crystals with nominal doping levels near the optimum one, two with $x = 0.096$ (#1 and #2), and one with $x = 0.098$ (#3). Their sizes are typically $1.5 \times 1.0 \times 0.3$ mm^3, being the c-axis of the tetragonal structure ($a = b = 3.96$ Å, $c = 12.77$ Å) perpendicular to their largest face. Details of their growth procedure and a thorough characterization may be found in [27].

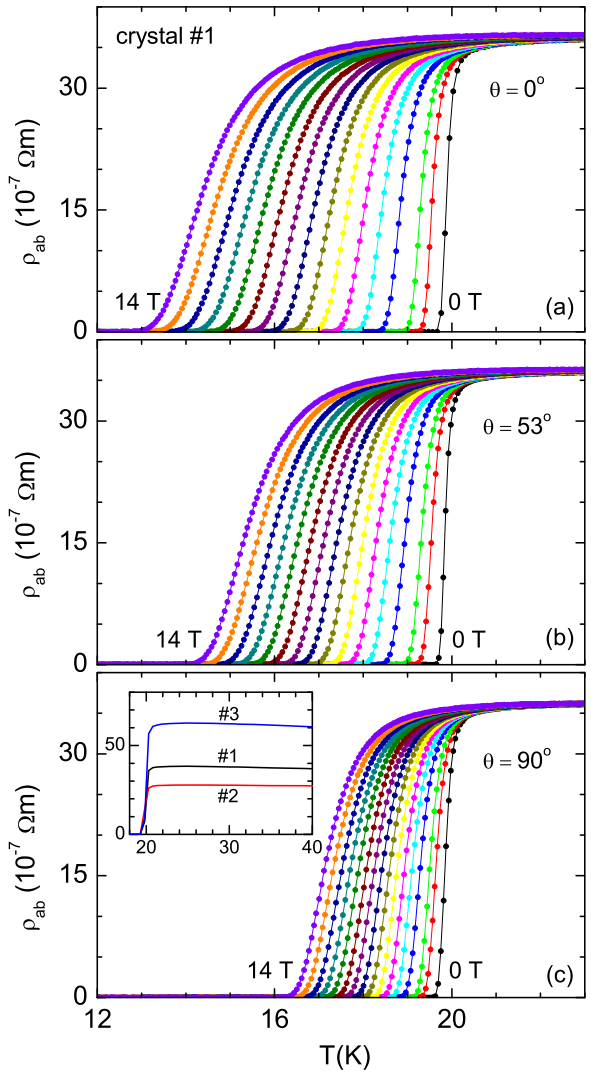

Figure 1. Temperature dependence of the resistivity around T_c for crystal #1. These measurements were performed in the presence of different magnetic field amplitudes (0, 0.5 T, and from 1 to 14 T in steps of 1 T) and orientations ($\theta = 0°$, 53°, and 90°) relative to the crystal c-axis. Inset in (c): overview up to $\sim 2T_c$ of the resistivity in the absence of a field for all the crystals studied.

The resistivity along the ab layers, ρ_{ab}, was measured with Quantum Design's Physical Property Measurement System (PPMS) in the presence of magnetic fields up to 14 T, with different orientations relative to the c-axis ($\theta = 0$, 53, and 90 degrees). We used a standard four-probe method with low-contact resistance (less than 1 Ohm) and a current of 1 mA. The data were obtained by sweeping the temperature at a rate of 0.3 K min^{-1}. An example of the $\rho_{ab}(T)_{H,\theta}$ behavior (corresponding to crystal #1) around T_c is presented in figure 1. The T_c value was determined from the transition midpoint for the $H = 0$ data, and the transition width was estimated as $\Delta T_c \approx T_c - T(\rho = 0)$. The corresponding values

[5] A theory for the effect of critical fluctuations around the $T_c(H)$ line on different observables in superconductors with intermediate 2D–3D characteristics was developed in [9].

Table 1. Summary of the superconducting parameters resulting from the analysis.

Crystal	T_c(K)	ΔT_c(K)	ξ_c (nm) ±6%	ξ_{ab} (nm) ±2%	γ ±8%
#1	19.8	0.3	1.28	2.57	2.00
#2	19.7	0.2	1.28	2.54	1.98
#3	19.8	0.2	1.24	2.52	2.02

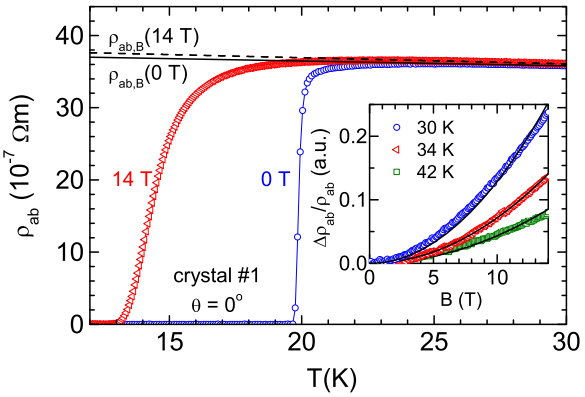

Figure 2. Temperature dependence of the resistivity around T_c for crystal #1, measured with $\mu_0 H = 0$ and 14 T perpendicular to the *ab* layers ($\theta = 0°$). The corresponding normal-state (or background) contributions (lines) were obtained by a linear fit above 26 K (i.e., 1.3 T_c), where fluctuation effects are expected to be negligible. Inset: field dependence of the magnetoresistivity, $\left[\rho_{ab}(B) - \rho_{ab}(0)\right]/\rho_{ab}(0)$, for several temperatures above T_c. The lines are fit to a quadratic form.

for the three samples studied are compiled in table 1. The small $\Delta T_c/T_c$ values (about 10^{-2}) confirm the excellent stoichiometric quality of the crystals. An overview of $\rho_{ab}(T)$ in the absence of a field and up to $\sim 2T_c$ is presented in the inset of figure 1(c) for all samples studied. As we can see, ρ_{ab} is almost temperature-independent from a few degrees above T_c up to $2T_c$. This is an important experimental advantage to determine the conductivity induced by superconducting fluctuations (or *paraconductivity*), which is given by

$$\Delta\sigma_{ab}(T, H) = \frac{1}{\rho_{ab}(T, H)} - \frac{1}{\rho_{ab,B}(T, H)}, \tag{1}$$

where $\rho_{ab,B}$ is the normal-state or *background* contribution. Figure 2 illustrates the procedure to estimate $\rho_{ab,B}$. In the region 26–30 K (corresponding to 1.3−1.5 T_c, where fluctuation effects are expected to be negligible [21]), the resistivity is linear with the temperature up to the largest field used in the experiments. Besides, as it is shown in the inset of that figure, the magnetoresistivity in the normal state is roughly quadratic in the applied magnetic field. This allows us to parametrize the background resistivity as

$$\rho_{ab,B}(T, H) = \alpha(H) + \beta(H)T, \tag{2}$$

where

$$\begin{aligned}\alpha(H) &= a_1 + a_2 H^2 \\ \beta(H) &= b_1 + b_2 H^2.\end{aligned} \tag{3}$$

The coefficients a_1, a_2, b_1, and b_2 were obtained by linear fittings to the $\rho_{ab}(T)$ curves measured with $\mu_0 H = 0$ and 14 T. An example (corresponding to crystal #1) of the resulting $\Delta\sigma_{ab}$ dependence on the reduced temperature, $\varepsilon \equiv \ln(T/T_c)$, is presented in figure 3.

3. Data analysis

3.1. In-plane paraconductivity in the low-field limit

In the absence of a magnetic field and for temperatures close to T_c, it is expected that $\Delta\sigma_{ab}$ will follow the classical AL result, which for 3D superconductors may be written as [28]

$$\Delta\sigma_{ab} = \frac{e^2}{32\hbar\xi_c}\varepsilon^{-1/2}, \tag{4}$$

where e is the electron charge, $\hbar$ is the reduced Planck constant, and ξ_c is the *c*-axis coherence length amplitude. As we see in the inset of figure 3, for reduced-temperatures below $\varepsilon \approx 0.1$, a critical exponent close to $-1/2$ is observed, in agreement with equation (4). Above this ε-value, a rapid falloff of the fluctuation effects is observed and a well-defined critical exponent is no longer observed, a behavior that may be attributed to short-wavelength fluctuation effects [2, 29, 30]. For completeness, in the same inset we present the prediction of the 2D-AL result

$$\Delta\sigma_{ab} = \frac{e^2}{16\hbar s}\varepsilon^{-1}, \tag{5}$$

where $s = 6.38$ Å is the periodicity length of the Fe-As layers. As we can clearly see, it overestimates the experimental data by almost two orders of magnitude, which is well beyond the experimental uncertainties, including those associated with the determination of the normal-state background.

In the presence of a finite magnetic field, roughly above the so-called *ghost critical field* $H^*(T)$ (which is the symmetric above T_c of the corresponding $H_{c2}(T)$ line [31]), $\Delta\sigma_{ab}$ is expected to be significantly reduced with respect to equation (4) [2, 32, 33]. As we see in figure 3, particularly in the $\Delta\sigma_{ab}(H)_\varepsilon$ representation of panels (d–f), such a reduction is clearly observed with the field amplitudes used in our experiments and, as expected, is more prominent for temperatures close to T_c (i.e., for $\varepsilon \to 0$). We also notice the dependence on the field orientation relative to the crystal's *c*-axis, which is a direct consequence of the anisotropy of the upper critical field in the studied compound (see below).

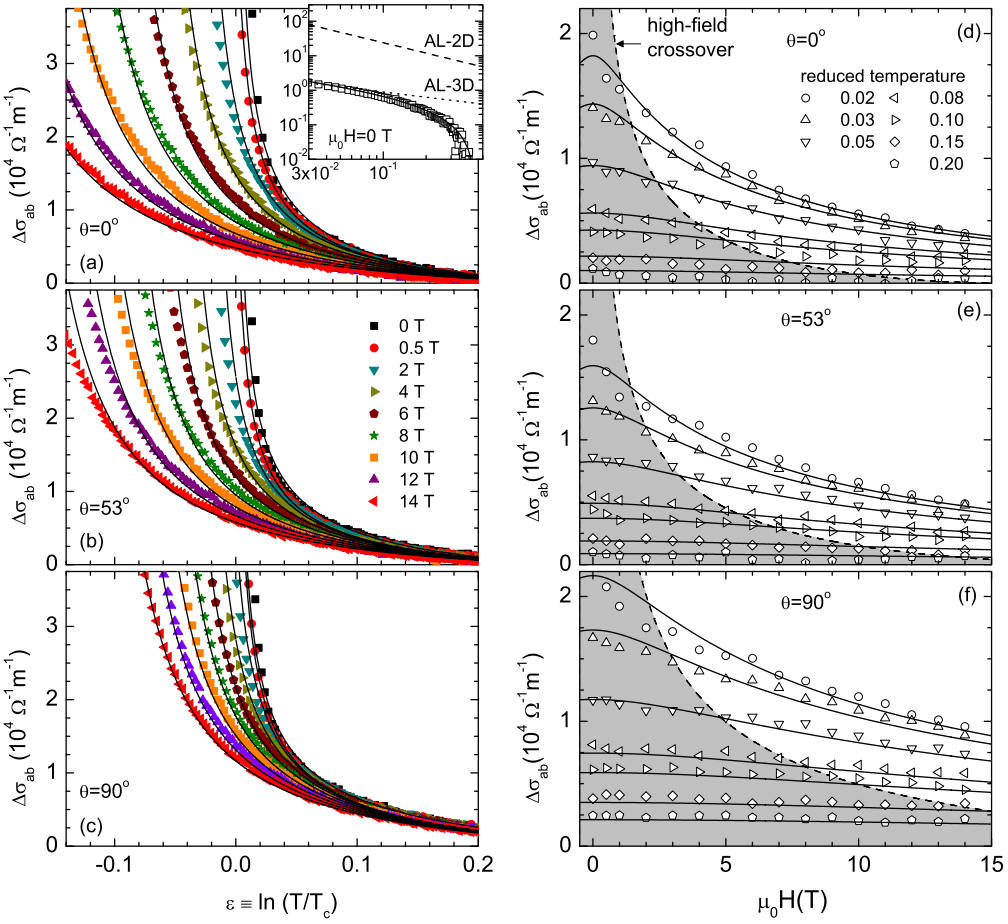

Figure 3. Example for crystal #1 of the $\Delta\sigma_{ab}$ dependence on the reduced temperature (a–c) and on the magnetic field amplitude (d–f). The indicated θ values represent the angle between the applied magnetic field and the crystal c-axis. The lines are the best fits for equation (6) using only three free parameters for the entire set of data of each field orientation: ξ_c, $H_{c2}(\theta)$, and C. The dashed lines in (d–f) represent the crossover to the Prange regime, according to the criterium $h = \varepsilon$. Inset in (a): log–log plot of the ε-dependence of $\Delta\sigma_{ab}$ in the absence of an applied field. Solid and dotted lines are the best fits for equation (6) and, respectively, the 3D-AL approach, equation (4) (this last for $\varepsilon < 0.1$, where short-wavelength effects are expected to be negligible). The dashed line is the prediction of the 2D-AL approach, equation (5).

3.2. Comparison with the GL approach for the finite-field or Prange regime

We will now analyze the experimental data in terms of the 3D-anisotropic GL approach developed in [21]. This approach adapts to the present dimensional case, the model proposed by A Schmid, which is based on a combination of the standard Gaussian GL-expression of the thermally-averaged current density with the generalized Langevin equation of the order parameter [34]. Since the energy of the fluctuation modes increases with H, this finite-field approach includes an energy cutoff in the fluctuation's spectrum as proposed in [29, 30]. For H perpendicular to the ab layers, it leads to

$$\Delta\sigma_{ab} = \frac{e^2}{32\hbar\pi\xi_c}\sqrt{\frac{2}{h}}\int_0^{\sqrt{\frac{C-\varepsilon}{2h}}} dx\left[\psi^1\left(\frac{\varepsilon+h}{2h}+x^2\right) - \psi^1\left(\frac{C+h}{2h}+x^2\right)\right], \quad (6)$$

where $h = H/H_{c2}^{\perp}$, $H_{c2}^{\perp}$ is the linear extrapolation to $T = 0$ K of the upper critical field for $H \perp ab$ (i.e., $\theta = 0°$), and C is a cutoff constant whose value is expected to be about ~0.5. [29, 30] In the zero-field limit (for $h \ll \varepsilon$, C), equation (6) is transformed into

$$\Delta\sigma_{ab} = \frac{e^2}{16\hbar\pi\xi_c}\left(\frac{\arctan\sqrt{\frac{C-\varepsilon}{\varepsilon}}}{\sqrt{\varepsilon}} - \frac{\arctan\sqrt{\frac{C-\varepsilon}{C}}}{\sqrt{C}}\right), \quad (7)$$

which at low reduced temperatures ($\varepsilon \ll C$) reduces to the conventional AL expression, equation (4). Following the scaling transformation for anisotropic materials developed in [35–37], equation (6) may be generalized to an arbitrary field orientation by just replacing h with

$$h_\theta = \frac{H}{H_{c2}(\theta)}, \quad (8)$$

$H_{c2}(\theta)$ being the upper critical field (linearly extrapolated to $T = 0$ K) for an arbitrary angle θ between **H** and the crystal c-axis.

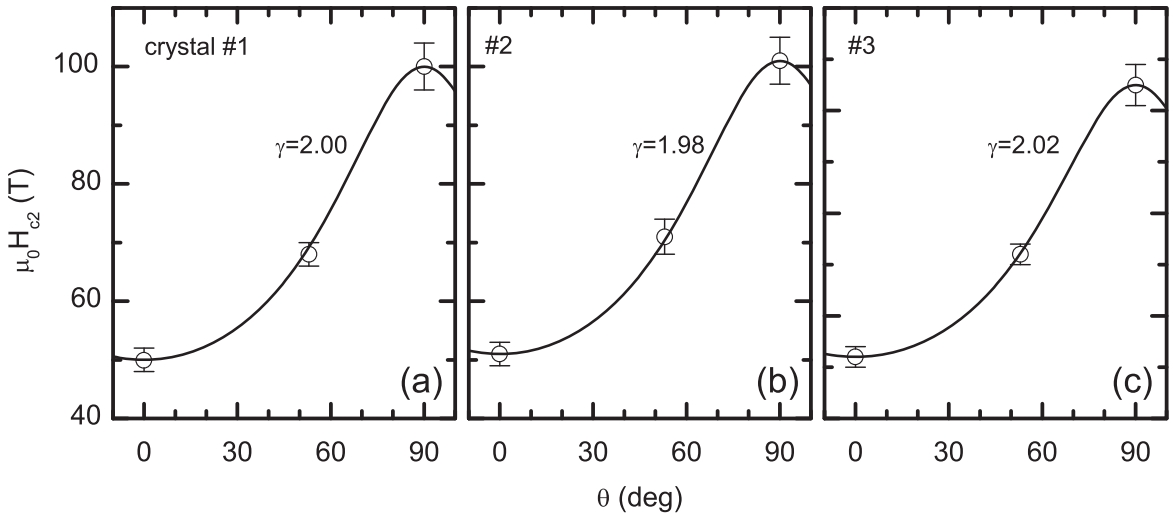

Figure 4. Dependence of H_{c2} on the angle between the applied field and the *c*-axis of the crystals. These data result from the analysis of $\Delta\sigma_{ab}(T, H)$ in the normal state in terms of equation (6). The lines correspond to the 3D-anisotropic GL expression, equation (9), evaluated by using the parameters in table 1.

Equation (6) is fitted to the complete set of data for each field orientation with only three free parameters: the upper critical field $H_{c2}(\theta)$, the amplitude (directly related to ξ_c), and the cutoff constant C. As we see in figure 3(a–c), the agreement is excellent, extending down to a field-dependent temperature below T_c that may be close to the upper bound of the *critical region*[6]. The agreement is also excellent in the $\Delta\sigma_{ab}(H)$ representation of figure 3(d–f), which is focused on temperatures above T_c. The resulting $H_{c2}(\theta)$ values are presented in figure 4 for all samples studied. These data follow the behavior expected for 3D-anisotropic materials (solid lines) [38],

$$H_{c2}(\theta) = \left[\frac{\cos^2\theta}{H_{c2}^2(0°)} + \frac{\sin^2\theta}{H_{c2}^2(90°)}\right]^{-1/2}, \qquad (9)$$

which represents an important consistency check of the present results. The $H_{c2}(0°)$ and $H_{c2}(90°)$ values are within the ones obtained in the literature in the same material from the shift of the resistive transition induced by the field [39–42], although the rounding associated with fluctuation effects makes this procedure strongly dependent on the criterion used (generally a given % of the normal-state resistivity). In the present case, as we see in figure 5, the 50% criterion gives H_{c2} values in good agreement with the ones resulting from the analysis of fluctuation effects.

As the $\Delta\sigma_{ab}$ amplitude may be affected by the uncertainties associated with both the finite size of the electrical contacts and the crystal's geometry, the amplitude term in equation (6) is not used to determine ξ_c. Instead, the GL coherence length amplitudes are obtained from the $H_{c2}(\theta)$ values in figure 4, according to

$$\xi_{ab} = \left[\frac{\phi_0}{2\pi\mu_0 H_{c2}(0°)}\right]^{1/2}, \qquad (10)$$

and

$$\xi_c = \xi_{ab}/\gamma, \qquad (11)$$

where the anisotropy factor γ is obtained from the ratio

$$\gamma = \frac{H_{c2}(90°)}{H_{c2}(0°)}. \qquad (12)$$

The values corresponding to each sample are compiled in table 1.

The resulting cutoff constant was in the range $C = 0.35 \pm 0.05$ for all samples. This value is close to that found in previous experiments on fluctuation effects above T_c in

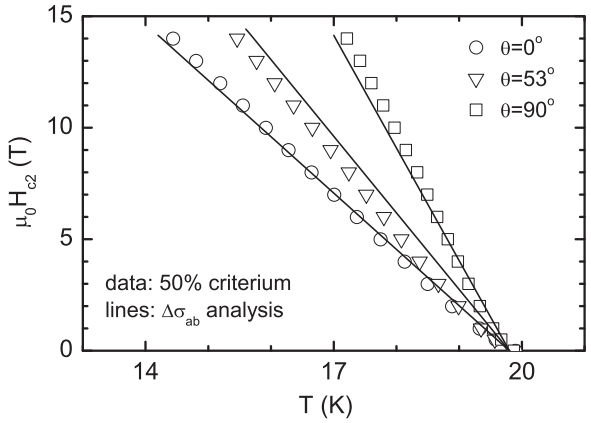

Figure 5. Temperature dependence of the upper critical field for the three field orientations studied, resulting from the analysis of fluctuation effects (lines) and from the 50% criterium (data points). The data of this example correspond to crystal #1. See the main text for details.

[6] In this region, fluctuation effects are so important that the Gaussian approximation [used to derive equation (6)] is no longer applicable. See [2].

FeSC, and in particular in experiments on the paraconductivity at high-ε values of the same compound [21], and on the precursor diamagnetism in optimally-doped $Ba_{1-x}K_xFe_2As_2$ [14]. It is also close to the cutoff constant found in other superconducting families, including high-T_c cuprates [43–46], low-T_c metallic elements and alloys [47, 48], and compounds like MgB_2or $NbSe_2$ [49, 50]. Our results confirm the proposal in [29, 30] about a universal C value close to ~0.5. This value is associated with the limits encountered at high-ε or h to the shrinkage of the superconducting wavefunction to lengths of the order of the pair size.

Let us finally comment on the applicability of a GL approach to a two-band superconductor as $BaFe_{2-x}Ni_xAs_2$. In principle, the analysis of fluctuation effects in multiband superconductors, in particular when they involve two or more weakly coupled bands with different anisotropy, would require a specific multiband functional that takes into account the non local effects arising from having an effective coherence length in one of the crystallographic directions of the system that is much smaller than the one associated with one of the bands. It has been proposed that this is the case with MgB_2 [51], although a good description of fluctuation effects in terms of GL approaches was also found for this compound [49]. The applicability of a GL approach to $BaFe_{2-x}Ni_xAs_2$ would suggest that the interband coupling in this compound is larger than that in MgB_2. This is consistent with the fact that the relative band interaction constant defined in [51], S_{12}, is in MgB_2 of the order of 0.035, while in optimally doped $BaFe_{2-x}Ni_xAs_2$ we find $S_{12} \simeq 0.134$ (i.e., four times larger) by using the coupling parameters reported in [52].

3.3. H–T phase diagram for $\Delta\sigma_{ab}$

The large number of measured $\Delta\sigma_{ab}$ isofields allowed us to plot detailed H–T phase diagrams of the $\Delta\sigma_{ab}$ amplitude for the three field orientations studied. An example for crystal #1 is shown in figure 6 . The solid line is the upper critical field, as obtained from the T_c and H_{c2} values in figure 4 by assuming a linear temperature dependence close to the transition. The dotted line represents the experimental limit of applicability of equation (6) which, as commented above, may be close to the onset of the *critical region*. In these phase diagrams, finite field effects may be seen as deviations from the verticality of the iso-$\Delta\sigma_{ab}$ curves. These effects are more prominent for $H\|c$ and, as expected, appear for fields roughly above the corresponding *ghost field*, $H^*(T)$. Finally, the circles indicate the points at which $\rho_{ab}(T)_H$ falls below the noise level, which are expected to be close to the irreversibility line, $H_{\rm irr}(T)$. It is worth noting that the dependence of $H_{\rm irr}(T)$ on the orientation of the applied magnetic field provides a further check of the applicability of the 3D-anisotropic GL approach to the compound under study. In fact, by approximating the irreversibility line by the melting line, according to [37] it is expected

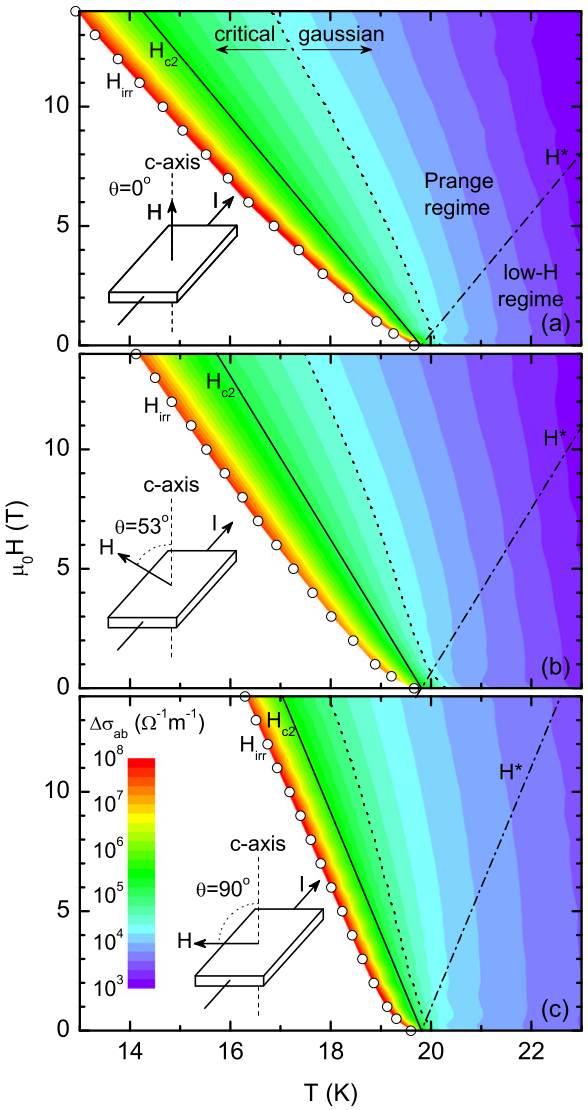

Figure 6. Experimental H–T phase diagram for crystal #1, showing the $\Delta\sigma_{ab}$ amplitude for the three **H** orientations studied. The circles indicate where the resistivity vanishes. The dotted line is the observed limit of applicability of equation (6), and roughly separates the *Gaussian* and *critical* fluctuation regimes. The solid line is the upper critical field resulting from the analysis of $\Delta\sigma_{ab}(T, H)$ in terms of equation (6). The dot-dashed line is the so-called *ghost field* (the symmetric above T_c of the upper critical field), above which finite field effects are expected to be relevant.

that

$$T_{\rm irr}(\mathbf{H}) = T_{\rm irr}\left(\frac{H}{H_{c2}(\theta)}\right). \qquad (13)$$

Then, taking into account equation (9), the $H_{\rm irr}(T)_\theta$ lines should scale when normalized by $\left(\cos^2\theta + \gamma^{-2}\sin^2\theta\right)^{-1/2}$. As we see in figure 7, such scaling is observed when using the γ values in table 1. Just for completeness, note that the irreversibility line for $\theta = 0°$ follows the temperature dependence predicted in [53], which was obtained within a 3D-disordered

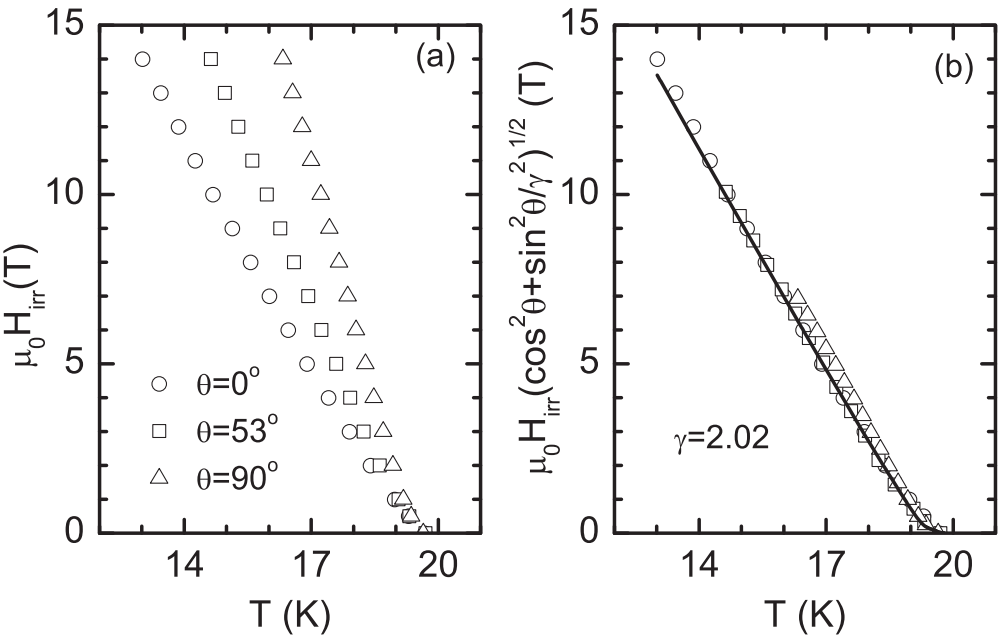

Figure 7. (a) Temperature dependence of the irreversibility field $H_{\rm irr}(T)$ for the three orientations of the applied field (this example corresponds to crystal #3). These data were obtained from the temperatures at which $\rho_{ab}(T)_{H,\theta}$ vanishes. (b) 3D-anisotropic GL scaling of the $H_{\rm irr}(T)_{H,\theta}$ data, evaluated by using the γ value in table 1. The line is the best fit of the theoretical approach presented in [53] (see main text for details).

GL model:

$$1 - t - h + 2\left[\frac{n_p(1-t)^2 h}{4\pi}\right]^{2/3} \times \left[\frac{3}{2} - \frac{4\pi t\sqrt{2Gi}}{n_p(1-t)^2}\right] = 0, \quad (14)$$

where $t = T/T_c$, $h = H/H_{c2}(\theta = 0°)$, and n_p and Gi are fitting parameters defined in [53], representing the disorder and the strength of thermal fluctuations, respectively. Values obtained from the fit are $\mu_0 H_{c2}(0°) = 42$ T, $n_p = 0.006$ and $Gi = 10^{-6}$. The value of n_p suggests that disorder is important in the reversible region below the $H_{c2}(T)$ line.

3.4. Comparison with recent works

In a recent work by Rullier-Albenque *et al* [20], it is reported that the paraconductivity of clean LiFeAs samples is 2D in nature, in spite of the fact that the superconducting parameters of this compound (similar to the ones of $BaFe_{2-x}Ni_xAs_2$) would suggest a 3D behavior: $\xi_c \sim 1.6$ nm is much larger than the interlayer distance, $s = 0.636$ nm. Here we show that this conflicting result may be an artifact associated with the procedure used to determine the normal-state contribution. First of all, let us note that in clean crystals the same fluctuation effects (i.e., the same $\Delta\sigma_{ab}$) lead to a much weaker resistivity rounding than in dirty samples (with a much larger background resistivity). The reason is that not too close to T_c, the change in the electrical resistivity due to superconducting fluctuations may be approximated by

$$\Delta\rho_{ab} \approx \rho_{ab,B}^2 \Delta\sigma_{ab}. \quad (15)$$

In the clean crystals used in [20], $\rho_{ab,B} \approx 4 \times 10^{-8}$ Ωm just above T_c. Subsequently, in the case of 3D fluctuations, at intermediate reduced temperatures (e.g., $\varepsilon = 0.1$) the relative change in ρ_{ab} is expected to be about 0.06%. Even in the case of 2D fluctuations, for which $\Delta\sigma_{ab}$ is given by equation (5), the relative change in ρ_{ab} is expected to be smaller than 1%. Indeed, the observation of fluctuation effects in the resistivity of clean crystals would require extraordinary precision in the determination of the background, whatever the procedure used. In [20], $\rho_{ab,B}$ is estimated by allegedly quenching fluctuation effects with magnetic fields typically above 10 T. However, it has been shown that fluctuations above T_c survive up to fields of the order of $T_c(dH_{c2}/dT)_{T_c}$ [33]. For LiFeAs this quantity is about 28 T [54], and it is likely that fluctuation effects are still present above 10 T.

Nevertheless, in [20] a good agreement (without free parameters) is found between equation (5) and the data obtained in one of the samples (named FP2). However, there is a large difference with the results obtained in the other sample (FP1): the $\Delta\sigma_{ab}$ data at 18.8 K ($\varepsilon \approx 0.09$), which is not included in figure 4 of [20] but is available from the data in figure 2(b), is a factor 2.5 larger than the one for sample FP2. The difference cannot be attributed to a wider superconducting transition (as is shown in figure 1(a), both samples present similar transition widths), and suggests that the

agreement of equation (5) with sample FP1 could be accidental. If the fluctuation effects in LiFeAs were actually 3D in nature, the arguments given in [20] supporting a pure H^2 behavior for transverse magnetoresistivity in this compound should be revised.

4. Conclusions

We have presented detailed measurements of the conductivity induced by superconducting fluctuations just above the superconducting transition of three high-quality, optimally doped $BaFe_{2-x}Ni_xAs_2$ single crystals. These measurements were performed with magnetic fields up to 14 T, which allowed us to deeply penetrate into the finite-field (or Prange) fluctuation regime. The magnetic field was applied with different orientations with respect to the crystal's *c*-axis ($\theta = 0°$, 53°, and 90°), allowing us to investigate the anisotropy of fluctuation effects. The analysis of the experimental data leads to solid evidence that a recently published Gaussian GL approach for 3D-anisotropic superconductors in the presence of finite applied magnetic fields applies to these compounds. Our results contrast with the recent observation of a seemingly 2D paraconductivity in clean LiFeAs single crystals, in spite of the fact that the coherence length amplitudes of this compound are similar to those in optimally doped $BaFe_{2-x}Ni_xAs_2$. The discrepancy may be attributed to the uncertainty in the normal-state contribution of the LiFeAs.

Acknowledgments

This work was supported by the Spanish MICINN and ERDF (No. FIS2010-19807), and by the Xunta de Galicia (Nos. 2010/XA043 and 10TMT206012PR). SSS and ADA acknowledge support from CNPq and FAPERJ. The work at IOP, CAS in China is supported by NSFC Program (No. 11374011) and MOST of China (973 project: 2011CBA00110).

References

[1] For reviews see
Johnston D C 2010 *Adv. Phys.* **59** 803
Mazin I I 2010 *Nature* **464** 183
Paglione J and Greene R 2010 *Nat. Phys.* **6** 645
Wang F and Lee D-H 2011 *Science* **332** 200
Stewart G R 2011 *Rev. Mod. Phys.* **83** 1589
[2] For an introductory review to the superconducting fluctuations, see
Tinkham M 1996 *Introduction to Superconductivity* (New York: McGraw-Hill) chapter 8
[3] Pallecchi I, Fanciulli C, Tropeano M, Palenzona A, Ferretti M, Malagoli A, Martinelli A, Sheikin I, Putti M and Ferdeghini C 2009 *Phys. Rev.* B **79** 104515
[4] Fanfarillo L, Benfatto L, Caprara S, Castellani C and Grilli M 2009 *Phys. Rev.* B **79** 172508
[5] Salem-Sugui S Jr, Ghivelder L, Alvarenga A D, Pimentel J L, Luo H-Q, Wang Z-S and Wen H-H 2009 *Phys. Rev.* B **80** 014518
[6] Choi C, Kim S H, Choi K-Y, Jung M-H, Lee S-I, Wang X F, Chen X H and Wang X L 2009 *Supercond. Sci. Technol.* **22** 105016
[7] Putti M *et al* 2010 *Supercond. Sci. Technol.* **23** 034003
[8] Liu S L, Haiyun W and Gang B 2010 *Phys. Lett.* A **374** 3529
[9] Murray J M and Tešanović Z 2010 *Phys. Rev. Lett.* **105** 037006
[10] Pandya S, Sherif S, Chandra L S S and Ganesan V 2010 *Supercond. Sci. Technol.* **23** 075015
[11] Kim S H, Choi C H, Jung M-H, Yoon J-B, Jo Y-H, Wang X F, Chen X H, Wang X L, Lee S-I and Choi K-Y 2010 *J. Appl. Phys.* **108** 063916
[12] Liu S L, Haiyun W and Gang B 2011 *Solid State Comm.* **151** 1
[13] Pandya S, Sherif S, Chandra L S S and Ganesan V 2011 *Supercond. Sci. Technol.* **24** 045011
[14] Mosqueira J, Dancausa J D, Vidal F, Salem-Sugui S Jr, Alvarenga A D, Luo H-Q, Wang Z-S and Wen H-H 2011 *Phys. Rev.* B **83** 094519
Mosqueira J, Dancausa J D, Vidal F, Salem-Sugui S Jr, Alvarenga A D, Luo H-Q, Wang Z-S and Wen H-H 2011 *Phys. Rev.* B **83** 219906(E)
[15] Welp U, Chaparro C, Koshelev A E, Kwok W K, Rydh A, Zhigadlo N D, Karpinski J and Weyeneth S 2011 *Phys. Rev.* B **83** 100513
[16] Liu S L, Longyan G, Gang B, Haiyun W and Yongtao L 2011 *Supercond. Sci. Technol.* **24** 075005
[17] Prando G, Lascialfari A, Rigamonti A, Romanó L, Sanna S A, Putti M and Tropeano M 2011 *Phys. Rev.* B **84** 064507
[18] Song Y J, Kang B, Rhee J-S and Kwon Y S 2012 *Europhys. Lett.* **97** 47003
[19] Marra P, Nigro A, Li Z, Chen G F, Wang N L, Luo J L and Noce C 2012 *New J. Phys.* **14** 043001
[20] Rullier-Albenque F, Colson D, Forget A and Alloul H 2012 *Phys. Rev. Lett.* **109** 187005
[21] Rey R I, Carballeira C, Mosqueira J, Salem-Sugui S Jr, Alvarenga A D, Luo H-Q, Lu X-Y, Chen Y-C and Vidal F 2013 *Supercond. Sci. Technol.* **26** 055004
[22] Salem-Sugui S Jr, Alvarenga A D, Rey R I, Mosqueira J, Luo H-Q and Lu X-Y 2013 *Supercond. Sci. Technol.* **26** 125019
[23] Mosqueira J, Dancausa J D, Carballeira C, Salem-Sugui S Jr, Alvarenga A D, Luo H-Q, Wang Z-S, Wen H-H and Vidal F 2013 *J. Supercond. Nov. Mag* **26** 1217
[24] For a review see
Vidal F and Ramallo M V 1998 The gap symmetry and fluctuations in high-T_c superconductors (*NATO Advanced Studies Institute, Series B: Physics*) ed J Bok, G Deutscher, D Pavuna and S A Wolf Vol 371 (New York: Plenum) p 443
[25] Bossoni L, Lascialfari A, Romanò L and Canfield P C arXiv:1311.1336
[26] Murphy J, Tanatar M A, Graf D, Brooks J S, Bud'ko S L, Canfield P C, Kogan V G and Prozorov R 2013 *Phys. Rev.* B **87** 094505
[27] Chen Y *et al* 2011 *Supercond. Sci. Technol.* **24** 065004
[28] Aslamazov L G and Larkin A I 1968 *Phys. Lett.* A **26** 238
[29] Vidal F, Carballeira C, Currás S R, Mosqueira J, Ramallo M V, Veira J A and Viña J 2002 *Europhys. Lett.* **59** 754
[30] Vidal F, Ramallo M V, Mosqueira J and Carballeira C 2003 *Int. J. Mod. Phys.* B **17** 3470
[31] Kapitulnik A, Palevski A and Deutscher G 1985 *J. Phys. C: Solid State Phys* **18** 1305
[32] Carballeira C, Mosqueira J, Revcolevschi A and Vidal F 2000 *Phys. Rev. Lett.* **84** 3157
Carballeira C, Mosqueira J, Revcolevschi A and Vidal F 2003 *Physica C* **384** 185

[33] Soto F, Carballeira C, Mosqueira J, Ramallo M V, Ruibal M, Veira J A and Vidal F 2004 *Phys. Rev.* B **70** 060501(R)
[34] Schmid A 1968 *Z. Phys.* **215** 210
Schmid A 1969 *Phys. Rev.* **180** 527
[35] Klemm R A and Clem J R 1980 *Phys. Rev.* B **21** 1868
[36] Blatter G, Geshkenbein V B and Larkin A I 1992 *Phys. Rev. Lett.* **68** 875
[37] Hao Z and Clem J R 1992 *Phys. Rev.* B **46** 5853
[38] Tinkham M 1996 *Introduction to Superconductivity* (New York: McGraw-Hill) p 321
[39] Sun D L, Liu Y and Lin C T 2009 *Phys. Rev.* B **80** 144515
[40] Tao Q, Shen J-Q, Li L-J, Lin X, Luo Y-K, Cao G-H and Xu Z-A 2009 *Chin. Phys. Lett.* **26** 097401
[41] Ni N, Thaler A, Yan J Q, Kracher A, Colombier E, Bud'ko S L, Canfield P C and Hannahs S T 2010 *Phys. Rev.* B **82** 024519
[42] Shahbazi M, Wang X L, Lin Z W, Zhu J G, Dou S X and Choi K Y 2011 *J. Appl. Phys.* **109** 07E151
[43] Mosqueira J, Cabo L and Vidal F 2009 *Phys. Rev.* B **80** 214527
[44] Mosqueira J, Cabo L and Vidal F 2007 *Phys. Rev.* B **76** 064521
[45] Mosqueira J and Vidal F 2008 *Phys. Rev.* B **77** 052507
[46] Mosqueira J, Carballeira C, Ramallo M V, Torrón C, Veira J A and Vidal F 2001 *Europhys. Lett.* **53** 632
[47] Mosqueira J, Carballeira C, Currás S R, González M T, Ramallo M V, Ruibal M, Torrón C and Vidal F 2003 *J. Phys: Condens. Matter* **15** 3283
[48] Mosqueira J, Carballeira C and Vidal F 2001 *Phys. Rev. Lett.* **87** 167009
[49] Mosqueira J, Ramallo M V, Currás S R, Torrón C and Vidal F 2002 *Phys. Rev.* B **65** 174522
[50] Soto F, Berger H, Cabo L, Carballeira C, Mosqueira J, Pavuna D and Vidal F 2007 *Phys. Rev.* B **75** 094509
[51] Koshelev A E, Varlamov A A and Vinokur V M 2005 *Phys. Rev.* B **72** 064523
[52] Rey R I, Ramos-Álvarez A, Mosqueira J, Salem-Sugui S Jr, Alvarenga A D, Luo H-Q, Lu X-Y, Zhang R and Vidal F 2014 *Supercond. Sci. Technol.* **27** 055015
[53] Rosenstein B and Zhuravlev V 2007 *Phys. Rev.* B **76** 014507
[54] Cho K, Kim H, Tanatar M A, Song Y J, Kwon Y S, Coniglio W A, Agosta C C, Gurevich A and Prozorov R 2011 *Phys. Rev.* B **83** 060502(R)